

**Growth rates of  
stratospheric  
HCFC-22**

D. P. Moore and  
J. J. Remedios

# Growth rates of stratospheric HCFC-22

**D. P. Moore and J. J. Remedios**

EOS, Space Research Centre, Department of Physics and Astronomy, University of Leicester,  
Leicester, LE1 7RH, UK

Received: 30 May 2007 – Accepted: 17 July 2007 – Published: 23 July 2007

Correspondence to: D. P. Moore (dpm9@le.ac.uk)

Title Page

Abstract

Introduction

Conclusions

References

Tables

Figures

⏪

⏩

◀

▶

Back

Close

Full Screen / Esc

Printer-friendly Version

Interactive Discussion

## Abstract

The Michelson Interferometer for Passive Atmospheric Sounding onboard ENVISAT (MIPAS-E) offers the opportunity to detect and spectrally resolve many atmospheric minor constituents affecting atmospheric chemistry. In this paper, we describe an algorithm produced to retrieve HCFC-22 profiles from MIPAS-E measurements made in 2003 and present results from this scheme between 300 and 50 mb. By comparison with ATMOS (AT-3) version 3 data, we find a mean Northern Hemisphere mid-latitude (20–50° N) HCFC-22 growth rate between 1994 and 2003 of  $5.4 \pm 0.7$  pptv/yr in the lower stratosphere (LS) and a mean LS Southern Hemisphere growth rate (60–80° S) of  $6.0 \pm 0.7$  pptv/yr in the same period. We test the feasibility of using a global data set to estimate the chemical lifetime of HCFC-22 in the LS and we derive this for two regions; 20–50° N ( $259 \pm 38$  years) and 60–80° S ( $288 \pm 34$  years). From these data we note a global LS lifetime of  $274 \pm 25$  years, significantly longer than previous estimates.

## 1 Introduction

In the early 1970s it was discovered that chlorofluorocarbons (CFCs), including CFC-11 ( $\text{CCl}_3\text{F}$ ) and CFC-12 ( $\text{CCl}_2\text{F}_2$ ), initiate strong stratospheric ozone depletion (Molina and Rowland, 1974). The CFCs are chemically inert in the troposphere and destroyed only in the stratosphere by photolysis. All of the chlorine contained in these compounds is released in the stratosphere and then initiates ozone depletion through a number of catalytic cycles. Hydrogenated CFCs (HCFCs) were seen as a viable alternative to CFCs due to their similar thermodynamic properties and, importantly, their primary sink is in the troposphere through oxidation with the hydroxyl radical (OH). This ultimately results in a lower flux of chlorine to the stratosphere (Cox et al., 1995) and therefore a lower impact on the ozone layer. Although the ozone depletion potential of HCFC-22 ( $\text{CHF}_2\text{Cl}$ ) is 20 times lower than that for CFC-12 (IPCC, 2001), it was decided that the production of all HCFCs also needed to be regulated. In 1990, the Montreal Protocol

### Growth rates of stratospheric HCFC-22

D. P. Moore and  
J. J. Remedios

Title Page

Abstract

Introduction

Conclusions

References

Tables

Figures

⏪

⏩

◀

▶

Back

Close

Full Screen / Esc

Printer-friendly Version

Interactive Discussion

(UNEP, 1996) set limits on HCFC production, with total phaseout planned in developed countries by 2030 and developing countries by 2040.

The major issue with the production and use of HCFC-22 is that it is an efficient greenhouse gas; it is 1700 times stronger as a greenhouse gas than an equivalent volume mixing ratio (vmr) of CO<sub>2</sub>. The radiative forcing of climate due to HCFC-22 is currently third amongst all halocarbons at 0.208 Wm<sup>-2</sup> ppbv<sup>-1</sup> (Sihra et al., 2001), behind only CFC-12 (0.32 Wm<sup>-2</sup> ppbv<sup>-1</sup>) and CFC-11 (0.24 Wm<sup>-2</sup> ppbv<sup>-1</sup>) in importance.

In January 2004, the global surface mean of HCFC-22 was 160 pptv (derived from NOAA Earth System Research Laboratory (ESRL) flask measurements) and increasing steadily at 5 pptv/yr. The reported production rate of HCFC-22 has recently begun to fall (AFEAS, 2003); between 1998 and 2002, the manufacture decreased by 8×10<sup>4</sup> metric tonnes. However, estimated surface emissions of HCFC-22 actually increased by 3×10<sup>4</sup> metric tonnes between 1998 and 2002. Tropospheric measurements made between 1987 and 2002 by Rinsland et al. (2005b) using a ground-based Michelson Interferometer at Kitt Peak in southern Arizona (31.9°N 111.6° W, 2.09 km altitude) show a linear rise in HCFC-22 concentrations of 5.66±0.15 pptv/yr, or 6.47±0.17%/yr over the whole of that period. The tropospheric lifetime of HCFC-22 has been determined from a number of studies (e.g. O'Doherty et al., 2004; Montzka and Fraser, 2003; Miller et al., 1998) and has been estimated to vary between 9 and 13 years.

The decadal lifetime of HCFC-22 in the troposphere allows troposphere-stratosphere mixing to occur and previous measurements made at Aire sur l'Adour, France, between 1982 and 1999 (Fabian and Borchers, 2001) showed the presence of HCFC-22 in the stratosphere; a mixing ratio that increased by 78 pptv at 20 km, during the 1982 to 1999 period. Over the coming decade atmospheric vmrs of HCFC-22 are expected to increase further as escape from refrigeration and air conditioning units continues. If Montreal Protocol targets are met, decay is then expected to occur, first detectable in the troposphere and then in the stratosphere. Hence, it is currently important to continue monitoring stratospheric concentrations of HCFC-22.

## Growth rates of stratospheric HCFC-22

D. P. Moore and  
J. J. Remedios

Title Page

Abstract

Introduction

Conclusions

References

Tables

Figures

⏪

⏩

◀

▶

Back

Close

Full Screen / Esc

Printer-friendly Version

Interactive Discussion

In this paper, we describe an algorithm produced to retrieve HCFC–22 profiles from measurements made by the Michelson Interferometer for Passive Atmospheric Sounding onboard ENVISAT (MIPAS-E), and present results from this scheme. We compare our results from 2003 to measurements made from ATMOS in 1994 in the Northern hemisphere mid-latitudes (20 to 50° N) in a manner similar to [Rinsland et al. \(2005a\)](#), and then extend our analyses to the Southern Hemisphere Polar region (60 to 80° S). From this we produce estimates of both the mid-latitude and Southern Hemisphere polar trends of HCFC–22 between 1994 and 2003. Finally, we calculate the lower stratospheric chemical lifetime of HCFC–22 at two locations; 20 to 50° N and 60 to 80° S.

## 2 MIPAS–E measurements of HCFC–22

The MIPAS–E instrument was successfully launched onboard the ENVIRONMENTAL SATellite (ENVISAT) in March 2002 as part of an ambitious and innovative payload. The ENVISAT is in a polar orbit at an altitude of 800 km, with an orbital period of about 100 min and a reference orbit repeat cycle of 35 days. The MIPAS–E ([Fischer and Oelhaf, 1996](#)) is a Fourier Transform Spectrometer that provides continual limb emission measurements in the mid infrared over the range 685–2410 cm<sup>-1</sup> (14.6–4.15 μm) at an unapodized resolution of 0.025 cm<sup>-1</sup>. The instrument’s field of view is approximately 3×30×400 km and one complete limb sequence of measurements in nominal mode consists of 17 spectra with tangent altitudes at 68 km, 60 km, 52 km, 47 km, 42 km and continuing downwards to 6 km in 3 km intervals.

### 2.1 Retrieval set-up

One of the main vibration-rotation transition features of HCFC–22 is the 2ν<sub>2</sub> band with an intense and very narrow Q–branch centred at 829.05 cm<sup>-1</sup> ([Varanasi, 1992](#)). The feature has been previously used to successfully retrieve HCFC–22 volume mixing

## Growth rates of stratospheric HCFC-22

D. P. Moore and  
J. J. Remedios

Title Page

Abstract

Introduction

Conclusions

References

Tables

Figures

⏪

⏩

◀

▶

Back

Close

Full Screen / Esc

Printer-friendly Version

Interactive Discussion

ratios (vmrs) from measurements made by the ATMOS instrument (e.g. [Rinsland et al., 2005a](#)).

The Oxford Reference Forward Model (RFM) was employed in order to model the observed spectra measured by MIPAS-E. The RFM is a line-by-line radiative transfer model, derived from the GenIn2 model ([Edwards, 1992](#)), with the ability to simulate infra-red spectra given the instrument lineshape, field-of-view, spectroscopic parameters and atmospheric composition profiles (see [www.atm.ox.ac.uk/RFM/](http://www.atm.ox.ac.uk/RFM/) for further details).

Figure 1 shows the contribution of HCFC-22 to the limb radiance measured by MIPAS-E between 828.95 and 829.15  $\text{cm}^{-1}$  at 12 and 21 km in the tropics (20° S to 20° N), as calculated using the line-by-line Oxford reference forward model (RFM). Profiles for pressure, temperature, HCFC-22 and all the interfering gases over the range were taken from the version 3.1 tropical reference atmospheres of [Remedios \(1999\)](#). Firstly, reference atmospheric limb emission spectra were calculated at a spectral resolution of 0.025  $\text{cm}^{-1}$  at 12 and 21 km including HCFC-22 and all other emitters in the region. To remove saturation effects, a second spectrum was calculated at the same resolution with all gases except HCFC-22. Differencing these two spectra leaves the radiance attributable to HCFC-22 only. The same method was used to determine the radiance contribution for each of the other interfering gases; the major contaminants include CFC-11,  $\text{C}_2\text{H}_6$ ,  $\text{CO}_2$ ,  $\text{H}_2\text{O}$  and  $\text{O}_3$ . The HCFC-22 signal is expected to exceed the MIPAS-E noise equivalent spectral radiance (NESR) between 828.95 to 829.15  $\text{cm}^{-1}$  at 12 km. At 21 km, however, the MIPAS-E noise equivalent spectral radiance (NESR) of 50  $\text{nW}/(\text{cm}^2 \text{sr cm}^{-1})$  ([Kleinert et al., 2007](#)) is much more important with only the peak of the 829.05  $\text{cm}^{-1}$  Q-branch visible above the NESR. The 828.95 to 829.15  $\text{cm}^{-1}$  region is therefore most suitable for retrievals from the upper troposphere and lowermost stratosphere.

The retrievals of HCFC-22 vmrs from MIPAS-E data have been achieved using the Optimal Estimation Retrieval Algorithm (OPERA), designed to invert MIPAS-E spectral measurements which is described in more detail in [Moore et al. \(2006\)](#). In essence, the

## Growth rates of stratospheric HCFC-22

D. P. Moore and  
J. J. Remedios

Title Page

Abstract

Introduction

Conclusions

References

Tables

Figures

◀

▶

◀

▶

Back

Close

Full Screen / Esc

Printer-friendly Version

Interactive Discussion

scheme uses the optimal estimation approach (Rodgers, 2000) to determine the most probable solution consistent with both the measurements and the a priori information.

Consider the set-up of the MIPAS-E, which makes  $m$  radiance measurements at different limb altitudes. A set of  $n$  parameters (the state vector  $\mathbf{x}$ ) are determined from this set of measurements  $\mathbf{y}$ . The aim of the retrieval is to gain as much information about  $\mathbf{x}$  given  $\mathbf{y}$ . The associated random error of the measurements, the measurement noise, is denoted by the vector  $\epsilon$ .

The relationship between the state vector and the measurement vector are related to a forward model,  $\mathbf{F}(x)$ , which attempts to approximate the atmospheric physics involved. Assuming a perfect model:

$$\mathbf{y} = \mathbf{F}(x) + \epsilon \quad (1)$$

The forward model incorporates knowledge of how the instrument works, coupled with how the measured quantity from the instrument (radiance for MIPAS-E) is related to the desired quantity (for example volume mixing ratios).

The remote sensing retrieval problem is non-linear and so simplifying assumptions are made to reduce the problem to a linear one. Optimal estimation (Rodgers, 2000) provides a linearized form for an estimate of  $\hat{\mathbf{x}}$  (the atmospheric profile) that is based on a prior estimate  $\mathbf{x}_a$  of the state and the set of measurements from the instrument:

$$\hat{\mathbf{x}} = \mathbf{G}\mathbf{y} + (\mathbf{I}_n - \mathbf{G}\mathbf{K})\mathbf{x}_a \quad (2)$$

where  $\mathbf{K}$  is the Jacobian matrix ( $K_{i,j} = \partial y_i / \partial x_j$ ) and  $\mathbf{G}$  is the gain matrix given by:

$$\mathbf{G} = \mathbf{S}_a \mathbf{K}^T (\mathbf{S}_y + \mathbf{K} \mathbf{S}_a \mathbf{K}^T)^{-1} \quad (3)$$

$\mathbf{S}_a$  is the covariance of  $\mathbf{x}_a$  about the exact state, and  $\mathbf{S}_y$  the covariance of  $\mathbf{y}$  about the perfect measurements that would arise from the exact state.

If the problem is not too non-linear then the Levenberg–Marquardt iteration technique can be used to find the best estimate of the state,  $\hat{\mathbf{x}}$ . The technique is similar to Gauss-Newton iteration but with the addition of an extra constant term,  $\gamma$ , which aids

**Growth rates of stratospheric HCFC-22**

D. P. Moore and  
J. J. Remedios

Title Page

Abstract

Introduction

Conclusions

References

Tables

Figures

⏪

⏩

◀

▶

Back

Close

Full Screen / Esc

Printer-friendly Version

Interactive Discussion

convergence. The value of  $\gamma$ , is initialised to a small value of one. If the value obtained from the iteration reduces the error, the new estimate,  $x_{i+1}$ , is accepted and  $\gamma$  is divided by ten. If the error increases on  $x_{i+1}$  however, then  $\gamma$  is multiplied by ten and Eq. (4) is solved again until an increment is obtained that reduces the error.

$$x_{i+1} = x_i + [(1 + \gamma)S_a^{-1} + K_i^T S_y^{-1} K_i]^{-1} \{K_i^T S_y^{-1} [y - F(x_i)] - S_a^{-1} [x_i - x_a]\} \quad (4)$$

where  $F$  is the RFM modelled radiance.

The OPERA performs a joint retrieval of HCFC–22 and total particle extinction on the same vertical grid as the measurements by calculating a mean spectral radiance at each altitude in two distinct regions; one sensitive to the target gas and the other to total particle extinction. This approach allows retrievals to be performed in the presence of thin cloud/aerosol in the upper troposphere. However, thicker clouds will still cause problems and so cloud flagging with a standard MIPAS-E technique was used.

Clouds were detected using a simple ratio approach by computing the ratio between the mean radiance in the 788.2 to 796.25  $\text{cm}^{-1}$  and 832.3 to 834.4  $\text{cm}^{-1}$  spectral bands (Spang et al., 2004) with a threshold value of 1.8. If ratios below this were found in a profile between 9 and 21 km the whole profile was flagged as cloudy, no retrieval performed on the scan and the scheme then analyzes the next scan. Pressure, temperature, water vapour, ozone and nitric acid vmrs, necessary in the forward model to compute both  $K$  and  $F$ , were taken from offline level 2 products from the MIPAS–E processor (version 4.61). A priori HCFC–22 vmr information was taken from the version 3.1 climatology files of (Remedios, 1999) with an assumed uncertainty of 100% on the profile. Volume mixing ratio information for other contaminants in the target gas and total extinction microwindows also came from the version 3.1 climatology files of Remedios (1999). Spectroscopic data were taken from HITRAN 2000 (Rothman et al., 2003).

**Growth rates of stratospheric HCFC-22**

D. P. Moore and J. J. Remedios

Title Page

Abstract

Introduction

Conclusions

References

Tables

Figures

⏪

⏩

◀

▶

Back

Close

Full Screen / Esc

Printer-friendly Version

Interactive Discussion

## 2.2 Retrieval errors

A detailed HCFC–22 error analysis is shown in Fig. 2 (random, systematic and total errors). The random errors comprised of retrieval noise and model parameter error. For the model parameter error, one sigma climatological uncertainties (Remedios, 1999) for the contaminants in the HCFC–22 microwindow were applied for each gas. Pressure and temperature uncertainties were assumed at 2% and 1 K respectively. The systematic model parameter errors were calculated using measured biases in MIPAS–E data. An uncertainty of 20% has been indicated for MIPAS–E water vapour (Lahoz et al., 2004), 10% for ozone (Kerridge et al., 2004) and 10% for nitric acid (Oelhaf et al., 2004). Uncertainties of 1 K for temperature (Dethof et al., 2004) and 2% for pressure were used. Although a systematic bias in the atmosphere files for the other contaminants was expected to be small, we assumed a 10% uncertainty for each of them. The errors due to uncertainties in these gases were likely to be lower in the real measurements than calculated here. The uncertainty of the instrument gain and instrument offset were taken to be 2% and  $2 \text{ nW}/(\text{cm}^2 \text{ sr cm}^{-1})$  respectively (Spang et al., 2005). Spectroscopic inaccuracies of HCFC–22 cross-section data were set to 3.5% (Clerbaux et al., 1993). For a single profile retrieval of HCFC–22, the random error dominates at all pressures in the upper troposphere and lowermost stratosphere (50 to 300 mb). The total error on a single retrieved vmr was below 50% at pressures above 100 mb. Systematic errors are dominated by spectroscopic uncertainties propagating into the retrieval. The error contribution due to other gases in the microwindow was dominated by uncertainties in CFC–11.

## 2.3 Retrieval characterization

There are many ways to characterise the data quality of a single profile retrieval such as averaging kernels, information content and the degrees of freedom for signal (dfs) of the measurement (Rodgers, 2000). The width of an averaging kernel determines the vertical resolution of a measurement and is also used to ascertain the information

### Growth rates of stratospheric HCFC-22

D. P. Moore and  
J. J. Remedios

Title Page

Abstract

Introduction

Conclusions

References

Tables

Figures

⏪

⏩

◀

▶

Back

Close

Full Screen / Esc

Printer-friendly Version

Interactive Discussion



content and degrees of freedom for a measurement. Fig. 3 shows a representative averaging kernel for a single mid-latitude profile of MIPAS–E data in 2003; HCFC–22 averaging kernels are strongly peaked above 0.4 in the upper troposphere and lower-most stratosphere. Between 50 and 300 mb (approximately 9 to 21 km) we generally observed between three and four degrees of freedom in the five MIPAS-E measurements in that height range; this information was highest at the summer pole (between 3.5 and 4) and lowest at the winter pole (between 2.5 and 3).

## 2.4 Processing of OPERA data

HCFC–22 retrievals were very sensitive to random error as there exists only nine spectral points in 828.95 to 829.15 cm<sup>-1</sup> microwindow. In the results section we have averaged profiles for the global mean and also by latitude band and as such the propagation of a priori information into the final result must be taken into account. A bias correction of up to 0.8% was applied for the a priori influence, following Burgess et al. (2004), where the measurement ( $\hat{\mathbf{m}}$ ) of the true atmosphere can be determined using the a priori ( $\mathbf{x}_a$ ), the defined a priori variance ( $\mathbf{S}_a$ ), the retrieved ( $\hat{\mathbf{x}}$ ) profiles and the retrieval error variance ( $\mathbf{S}_x$ ) information:

$$\hat{\mathbf{m}} = (\hat{\mathbf{x}}/\mathbf{S}_x) - (\mathbf{x}_a/\mathbf{S}_a)(1/\mathbf{S}_x - 1/\mathbf{S}_a)^{-1} \quad (5)$$

## 3 Results

Although surface measurements of HCFC–22 vmrs are routinely performed (e.g. the ESRL surface network, Montzka et al., 1993), measurements of HCFC–22 vmrs in the upper troposphere and lower stratosphere are generally limited to infrequent balloon or aircraft measurement campaigns. Solar occultation limb measurements by ATMOS (Gunson et al., 1996) or more recently from ACE (Bernath et al., 2005) have provided valuable information on the vertical profile of HCFC–22 but global coverage is only achieved in these cases if many months of data are combined. The MIPAS–E has

### Growth rates of stratospheric HCFC-22

D. P. Moore and  
J. J. Remedios

Title Page

Abstract

Introduction

Conclusions

References

Tables

Figures

◀

▶

◀

▶

Back

Close

Full Screen / Esc

Printer-friendly Version

Interactive Discussion

provided global limb measurements of the atmosphere since September 2002 albeit with interruptions due to ice decontamination and problems with the interferometer slides.

For this study we have retrieved HCFC–22 vmrs and total particle extinctions from one week of data from each season in 2003; these data were recorded at high spectral resolution ( $0.025\text{ cm}^{-1}$ ). Weeks were chosen that had very good data availability for both the measured level 1b (calibrated and geolocated) spectra and offline (version 4.62) level 2 data for pressure, temperature, water vapor, nitric acid and ozone. Zonal mean profile results are shown from 8 to 14 January (2192 profiles), 15 to 21 April (1295 profiles), 8 to 14 July (711 profiles) and 15 to 21 October (2236 profiles).

### 3.1 Zonal Mean Profiles

The global mean profile from the 6434 converged profiles from 2003 is shown in Fig. 4. Although data were retrieved at five MIPAS–E measurement levels between 9 and 21 km, we decided to only show data where more information was gained from the measurement than the a priori knowledge, see Sect. 2.3. The global mean data display both a tropospheric and stratospheric component; as HCFC–22 is purely anthropogenic in origin the decrease in vmr with increasing altitude is due to increasing photolysis.

The global mean surface vmr of HCFC–22 for 2003 (derived from ESRL flask measurements) was 158 pptv. This compares quite well with the mean MIPAS-E global profile at 300 mb of  $177 \pm 17.5$  pptv where the error is the systematic uncertainty; the random error on the mean at 300 mb was 0.5 pptv. It is important to note that our data are only slightly Northern Hemisphere (NH) biased (56% of data points, 3590 profiles) compared to the Southern Hemisphere (SH) (2844 profiles). It has been shown by [Waugh and Hall \(2002\)](#) that there is an interhemispheric variation in gas concentrations with an anthropogenic source; interhemispheric transport takes around one year. For a gas such as HCFC–22, with an annual growth rate of 5 pptv/yr, the mean NH tropospheric HCFC–22 vmr in 2003 was 166 pptv compared to 150 pptv in the SH (based on ESRL flask measurements).

## Growth rates of stratospheric HCFC-22

D. P. Moore and  
J. J. Remedios

Title Page

Abstract

Introduction

Conclusions

References

Tables

Figures

⏪

⏩

◀

▶

Back

Close

Full Screen / Esc

Printer-friendly Version

Interactive Discussion

Due to the large number of retrieved data we also investigated latitudinal variability of HCFC-22 with the results overlaid in Fig. 4. In particular, the polar data show good agreement in profile shape but at 300 mb the Northern Polar mean was 8 pptv higher than the Antarctic mean. Mid-latitude data also showed good profile shape agreement with no systematic hemispheric differences; however, below the 200 mb pressure level the mean NH HCFC-22 vmr is 5 pptv greater than in the SH. Finally tropical data, although expected to be mostly tropospheric and therefore show no decrease in HCFC-22 over the measured levels, does show some unexpectedly high HCFC-22 vmrs at approximately 150 mb of over 195 pptv. The exact cause of this anomalously high HCFC-22 is not known although the 150 mb tropical retrieval is very sensitive to uncertainties in pressure and temperature. We therefore do not use tropical data in the following trend analysis and lifetime calculations.

### 3.2 Trend analysis

As outlined in the introduction, the global surface vmr of HCFC-22 has been monitored since 1992, through the ESRL, with a near-linear rise of 5.2 pptv/yr measured between 1992 and January 2004. There have been several studies (e.g. Miller et al., 1998; O'Doherty et al., 2004; Irion et al., 1994; Rinsland et al., 2005b) to monitor the tropospheric growth rate of HCFC-22 from individual surface stations. Little is known, however, about the stratospheric growth rate of HCFC-22.

We have calculated the average stratospheric growth rate of HCFC-22 by comparing target vmrs with N<sub>2</sub>O for both ATMOS (version 3 data; 3 to 14 November 1994) and MIPAS-E (version 4.61 data; 15 to 21 October 2003). Elkins et al. (2004) used NOAA/ESRL measurements of N<sub>2</sub>O vmrs to calculate a tropospheric 2003 global mean of 318 ppbv; therefore, we assume that where MIPAS-E N<sub>2</sub>O vmrs are less than 318 ppbv, the measurements are likely be stratospheric. MIPAS-E N<sub>2</sub>O has a precision of ±10% and shows a positive bias with respect to several types of correlative measurements in the UTLS at pressures greater than 100 mb (Camy-Peyret et al., 2004). As such, we believe a 318 ppbv cut-off is conservative for this purpose but as-

## Growth rates of stratospheric HCFC-22

D. P. Moore and  
J. J. Remedios

Title Page

Abstract

Introduction

Conclusions

References

Tables

Figures

⏪

⏩

◀

▶

Back

Close

Full Screen / Esc

Printer-friendly Version

Interactive Discussion

sign an error of 10% between 20 and 50° N and 5% between 60 and 80° S for MIPAS-E N<sub>2</sub>O based on a direct comparison of mean N<sub>2</sub>O with expected tropospheric values (R. Leigh, personal communication).

We report the average lower stratospheric growth rate of HCFC–22 between 1994 and 2003 for both the NH mid-latitudes (20° N to 50° N) and, for the first time, the SH polar region (60° S to 80° S). Our analysis extends between 300 and 50 mb for each region, a critical region in terms of climate study, where the vmr of HCFC–22 is expected to decrease with height (Fabian and Borchers, 2001). Only data at heights with significant measurement information (determined from the dfs) were included and these data were corrected for a priori bias (Sect. 2.4).

Figure 5 compares ATMOS HCFC–22 and N<sub>2</sub>O data with MIPAS–E HCFC–22 and N<sub>2</sub>O between 20°N to 50° N. The HCFC–22 vmrs were binned by 5 ppbv N<sub>2</sub>O increments, averaged, the standard error of each bin determined and displayed in Fig. 5. A total of 941 MIPAS–E data points and 238 ATMOS data points of HCFC–22 have been included for this comparison. It has been calculated that the systematic errors dominate our HCFC–22 error estimate and are of the order of 5% for HCFC–22 from MIPAS–E in the mid-latitudes (50 to 300 mb). The version 3 ATMOS data for HCFC–22 have a quoted accuracy of 11% and for N<sub>2</sub>O 5% over the same pressure range (Abrams et al., 1996).

From these data, we have derived an average HCFC–22 growth rate of  $5.4 \pm 0.7$  pptv/yr ( $3.5 \pm 0.4\%$ /yr) in the mid-latitude stratosphere (20 to 50° N) between 1994 and 2003. Our measured percentage growth rate compares fairly well, although slightly lower, with the  $3.92 \pm 2.08$  %/yr determined by Rinsland et al. (2005a) who compared stratospheric ATMOS–3 (1994) and ACE (2004) HCFC–22 near 30° N. Our comparisons for the mid-latitudes are similar to ACE as they cover an equivalent range of altitudes.

We also report, for the first time, a Southern Hemisphere growth rate of HCFC–22 in the lower stratosphere (60° S to 80° S), Fig. 6. Using the same technique as for the mid-latitude estimate and measurements over the same pressure range (420 MIPAS–E

## Growth rates of stratospheric HCFC-22

D. P. Moore and  
J. J. Remedios

[Title Page](#)[Abstract](#)[Introduction](#)[Conclusions](#)[References](#)[Tables](#)[Figures](#)[⏪](#)[⏩](#)[◀](#)[▶](#)[Back](#)[Close](#)[Full Screen / Esc](#)[Printer-friendly Version](#)[Interactive Discussion](#)

data, 286 ATMOS data), we estimated an average yearly growth rate in HCFC–22 of  $6.0 \pm 0.7$  pptv/yr ( $4.3 \pm 0.5$  %) between 1994 and 2003. Considering that the age of air at 20 km between 60 and 80° S is on average around 4.5 years (Andrews et al., 2001) our stratospheric growth rate is likely to be similar to the tropospheric trend between 1989 and 1998. A regular observation program of tropospheric HCFC–22 vmrs have been carried out at Cape Grim, Tasmania (40° S, 144° E) since April 1978. Miller et al. (1998) report a SH tropospheric growth rate from this station in 1992 of  $5.5 \pm 0.1$  pptv/yr, slightly lower than our 1994 to 2003 measurement. By mid-1996 however Miller et al. (1998) report an increase in the Cape Grim HCFC–22 trend to  $6.0 \pm 0.1$  pptv/yr, more consistent with our measurements. Our SH growth rate is 0.6 pptv/yr greater than that we measured in the NH, but the errors overlap.

The gradient of the fit to HCFC–22 and N<sub>2</sub>O shown in Figs. 5 and 6 is related to the chemical lifetime of both species. The basis of the Plumb and Ko (1992) approach to estimating the chemical lifetime relies in the fact that long-lived species in the stratosphere exhibit an 'equilibrium slope' determined by a balance between photochemical changes and transport processes. As the local stratospheric lifetimes of N<sub>2</sub>O and HCFC–22 are longer than the timescale for horizontal transport, their correlation is compact (Figs. 5 and 6). The linear correlation obtained gives the ratio of their lifetimes via:

$$\frac{\tau_1}{\tau_2} \cong \frac{d\sigma_2}{d\sigma_1} \frac{\sigma_1}{\sigma_2} \quad (6)$$

where  $\tau_1$  and  $\tau_2$  are the lifetimes of gas 1 (here HCFC–22) and gas 2 (N<sub>2</sub>O) respectively,  $\sigma_1$  and  $\sigma_2$  are the (mean) mixing ratios of HCFC–22 and N<sub>2</sub>O respectively and  $d\sigma_2/d\sigma_1$  is the slope of the linear correlation. We have tested this theory related to reprocessed MIPAS-E N<sub>2</sub>O (version 4.61) and OPERA retrieved HCFC–22 from MIPAS–E I1b spectra (version 4.61) and have estimated a global average lifetime of HCFC–22 in the lowermost stratosphere.

Assuming an atmospheric lifetime of N<sub>2</sub>O of 120 years (IPCC, 2001), using only stratospheric data (N<sub>2</sub>O less than 318 pptv) at pressures between 50 and 300 mb,

## Growth rates of stratospheric HCFC-22

D. P. Moore and  
J. J. Remedios

[Title Page](#)[Abstract](#)[Introduction](#)[Conclusions](#)[References](#)[Tables](#)[Figures](#)[⏪](#)[⏩](#)[◀](#)[▶](#)[Back](#)[Close](#)[Full Screen / Esc](#)[Printer-friendly Version](#)[Interactive Discussion](#)

we calculate a NH mid-latitude (20 to 50° N) stratospheric lifetime of HCFC–22 of  $259 \pm 38$  years increasing to  $288 \pm 34$  years in Antarctica (60 to 80° S). The uncertainty on the lifetime is calculated from the standard error of the least square polynomial fit and the estimated accuracy of the MIPAS–E HCFC–22 and N<sub>2</sub>O data. Within errors, the difference between these two estimates are not significant. Since, within the errors, the two results overlap, we infer a global stratospheric lifetime of approximately  $274 \pm 25$  years. These two estimates of stratospheric HCFC–22 lifetime we derive are higher than the modeled global lifetimes derived by [Avallone and Prather \(1997\)](#) [205 years], [Kanakidou et al. \(1995\)](#) [214 years] and [Spivakovsky et al. \(2000\)](#) [229 years]. We therefore confirm that the stratospheric lifetime of HCFC–22 is significant and could be longer than previous estimates. Finally, the ratio of the HCFC–22 lifetime to that of N<sub>2</sub>O is between 2.2 (20 to 50° N) and 2.4 (60 to 80° S).

## 4 Conclusions

HCFC–22 is both an important greenhouse gas ([IPCC, 2001](#)) and contributes to stratospheric ozone depletion ([UNEP, 1996](#)). Although a critical gas, previous stratospheric measurements have been limited to infrequent balloon campaigns or solar occultation missions which provide limited latitude coverage of data. Regular monitoring of the global lower stratospheric distribution of HCFC–22 is now feasible due to the advent of instruments such as the MIPAS–E measuring limb thermal emission.

This work has demonstrated the ability of the OPERA scheme to retrieve HCFC–22 vmrs from single scans of MIPAS–E spectral data between 9 and 21 km, with 3–4 degrees of freedom for each profile from five measurement levels. Averaging single profiles from many orbits reduced the random errors considerably and the major error source arose from systematic errors; particularly inaccuracies in the HCFC–22 spectroscopy used in the forward model. The yearly mean polar profile in 2003 shows distinct tropospheric ( $173.1 \pm 10.9$  pptv) and stratospheric ( $141.6 \pm 7.7$  pptv) components. The same is true of the yearly mean mid-latitude profile with tropospheric

### Growth rates of stratospheric HCFC-22

D. P. Moore and  
J. J. Remedios

Title Page

Abstract

Introduction

Conclusions

References

Tables

Figures

⏪

⏩

◀

▶

Back

Close

Full Screen / Esc

Printer-friendly Version

Interactive Discussion

( $174.5 \pm 11.8$  pptv) and lowermost stratosphere ( $162.2 \pm 8.2$  pptv) components. There are some unresolved issues with high HCFC-22 vmrs in the tropics compared to surface observations. This may be due to inaccuracies in the retrieved temperature and/or pressure data used which propagates through the scheme into HCFC-22 vmr errors.

5 This is in the process of further investigation.

We have shown that MIPAS-E data can be compared to another, independent, satellite dataset to infer lower stratospheric trends in HCFC-22 vmrs. By comparison to ATMOS (AT-3) version 3 data from November 1994 we have estimated a NH mid-latitudes (20 to 50° N) HCFC-22 growth rate HCFC-22 of  $5.4 \pm 0.7$  pptv/yr ( $3.5 \pm 0.4\%$ /yr) between 1994 and 2003; which compares well with the stratospheric NH 25 to 35° N growth of  $3.92 \pm 2.08\%$ /yr rate estimated by [Rinsland et al. \(2005a\)](#) between 1994 and 2004.

We have also calculated, for the first time, a mean lower stratosphere HCFC-22 growth rate for the Southern Hemisphere polar regions (60 to 80° S). Between 1994 and 2003, we measured an increase of  $6.0 \pm 0.7$  pptv/yr ( $4.3 \pm 0.5\%$ /yr). We also note that our SH rate of increase is just over 0.6 pptv/yr higher than our measured NH average.

We have tested the feasibility of using a global data set of remotely sensed MIPAS-E data to measure the lifetime of HCFC-22 in the lowermost stratosphere. We derive the stratospheric lifetime of HCFC-22 at two locations; 20 to 50° S ( $259 \pm 38$  years) and 60 to 80° S ( $288 \pm 34$  years). Since the two sets of error bars overlap, we note a global stratospheric lifetime of approximately  $274 \pm 25$  years. These estimates are higher than global stratospheric lifetimes estimated by various chemistry models (205 to 229 years).

25 Our work confirms that current satellite systems are highly suitable for trend monitoring of HCFC-22 in the stratosphere. There remains a need to continue monitoring the stratosphere to verify that future reductions in atmospheric loading, in response to restrictions on HCFC-22 production in the Montreal Protocol, are realized. Future work will likely involve monitoring the stratospheric trend of HCFC-22 from compar-

**Growth rates of stratospheric HCFC-22**

D. P. Moore and J. J. Remedios

Title Page

Abstract

Introduction

Conclusions

References

Tables

Figures

⏪

⏩

◀

▶

Back

Close

Full Screen / Esc

Printer-friendly Version

Interactive Discussion



ison of different years of MIPAS–E data, extending further the availability to monitor global trends. This work also suggests that the global capabilities of MIPAS–E data would allow identification of latitudinal stratospheric trends of trace gases with stronger variations of tropospheric growth rates.

5 *Acknowledgements.* D. Moore was supported by a research studentship from the Natural Environment Research Council. The authors wish to thank the European Space Agency for access to MIPAS data under CUTLSOM (AO–357). The authors would also like to thank the NOAA Earth System Research Laboratory Halocarbons and other atmospheric trace species group for making HCFC–22 flask data publically available via their website  
10 (<http://www.esrl.noaa.gov/gmd/hats/>).

## References

Abrams, M. C., Chang, A. C., Gunson, M. R., Abbas, M. M., Goldman, A., Irion, F. W., Michelson, H. A., Newchurch, M. J., Rinsland, C. P., Stiller, G. P., and Zander, R.: On the assessment and uncertainty of atmospheric trace gas burden measurements with high resolution  
15 infrared solar occultation spectra from space by the ATMOS experiment, *Geophys. Res. Lett.*, 23(17), 2337–2340, 1996. [10526](#)

AFEAS (Alternative Fluorocarbons Environmental Acceptability Study): Production, Sales and calculated emissions of Fluorocarbons through 2001, <http://www.afeas.org>, 2003. [10517](#)

20 Andrews, A. E., Boering, K. A., Daube, B. C., Wofsy, S. C., Loewenstein, M., Jost, H., Podolske, J. R., Webster, C. R., Herman, R. L., Scott, D. C., Flesch, G. J., Moyer, E. J., Elkins, J. W., Dutton, G. S., Hurst, D. F., Moore, F. L., Ray, E. A., Romashkin, P. A., and Strahan, S. E.: Mean ages of stratospheric air derived from in situ observations of CO<sub>2</sub>, CH<sub>4</sub>, and N<sub>2</sub>O, *J. Geophys. Res.*, 106(D23), 32 295–32 314, 2001. [10527](#)

25 Avallone, L., and Prather, M.: Tracer-tracer correlations: Three-dimensional model simulations and comparisons to observations, *J. Geophys. Res.*, 102(D15), 19 233–19,246, doi:10.1029/97JD01123, 1997. [10528](#)

Bernath, P. F., McElroy, C. T., Abrams, M. C., Boone, C. D., Butler, M., Camy-Peyret, C., Carleer, M., Clerbaux, C., Coheur, P.-F., Colin, R., DeCola, P., Gilbert, K., Jennings, D. E., Llewellyn, E. J., Lowe, R. P., Mathieu, E., McConnell, J. C., McHugh, M., McLeod, S. D., Michaud, R.,

## Growth rates of stratospheric HCFC-22

D. P. Moore and  
J. J. Remedios

Title Page

Abstract

Introduction

Conclusions

References

Tables

Figures

◀

▶

◀

▶

Back

Close

Full Screen / Esc

Printer-friendly Version

Interactive Discussion



**Growth rates of  
stratospheric  
HCFC-22**D. P. Moore and  
J. J. Remedios

Title Page

Abstract

Introduction

Conclusions

References

Tables

Figures

⏪

⏩

◀

▶

Back

Close

Full Screen / Esc

Printer-friendly Version

Interactive Discussion

Midwinter, C., Nassar, R., Nichitiu, F., Nowlan, C., Rinsland, C. P., Rochon, Y. J., Rowlands, N., Semeniuk, K., Simon, P., Skelton, R., Sloan, J. J., Soucy, M.-A., Strong, K., Tremblay, P., Turnbull, D., Walker, K. A., Walkty, I., Wardle, D. A., Wehrle, V., Zander, R., and Zou, J.: Atmospheric Chemistry Experiment (ACE): Mission overview, *Geophys. Res. Lett.*, 32, L15S01, doi:10.1029/2005GL022386, 2005. [10523](#)

Burgess, A. B., Grainger, R. G., Dudhia, A., and Payne V. H.: MIPAS measurements of sulphur hexafluoride (SF<sub>6</sub>), *Geophys. Res. Lett.*, 31, L05112, doi:10.1029/2003GL019143, 2004. [10523](#)

Camy-Peyret, C., Dufour, G., Payan, S., Oelhaf, H., Wetzell, G., Stiller, G. P., Blumenstock, T., Blom, C. E., Gulde, T., Glatthor, N., Engel, A., Pirre, M., Catoire, V., Moreau, G., De Maziere, M., Vigouroux, C., Mathieu, E., Cortesi, U., and Mencaraglia F.: Validation of MIPAS N<sub>2</sub>O profiles by stratospheric balloon, aircraft and ground based measurements, Proceedings of the ACVE-2 meeting, 3–7 May, Frascati, Italy, 2004. [10525](#)

Clerbaux, C., Colin, R., Simon, P., and Granier C.: Infrared cross-sections and global warming potentials of 10 alternative hydrohalocarbons, *J. Geophys. Res.*, 98, 10 491–10 497, 1993. [10522](#)

Cox, R., Atkinson, R., Moortgat, G. K., Ravishankara, A. R., and Sidebottom, H. W.: Atmospheric degradation of halocarbon substitutes, in *Scientific Assessment of Ozone Depletion*, edited by D. L. Albritton, R. T. Watson, and P. J. Aucamp, vol. 37, report, pp. 12.1–12.23, World Meteorol. Org., Geneva, 1995. [10516](#)

Dethof, A., Geer, A., Lahoz, W., Goutail, F., Bazureau, A., Wang, D.-Y., and von Clarmann, T.: MIPAS temperature validation by the MASI group, Proceedings of the ACVE-2 meeting, 3–7 May, Frascati, Italy, 2004. [10522](#)

Edwards, D. P.: GENLN2: A general line-by-line atmospheric transmittance and radiance model, Version 3.0 description and users guide, NCAR/TN-367-STR, National Center for Atmospheric Research, Boulder, Co, 1992. [10519](#)

Elkins, J. W., Dutton, G. S., Hall, B. D., Butler, J. H., Thompson, T. M., Mondeel, D. J., and Dlugokencky, E. J.: Global trends and distributions of atmospheric nitrous oxide, *Eos Trans. AGU, Fall Meet. Suppl.*, Abstract A51C–0779, 2004. [10525](#)

Fabian, P., and Borchers, R.: Growth of Halocarbon Abundances in the Stratosphere between 1977 and 1999, *Adv. Space. Res.*, 28(7), 961–964, 2001. [10517](#), [10526](#)

Fischer, H., and Oelhaf, H.: Remote sensing of vertical profiles of atmospheric trace constituents with MIPAS limb-emission spectrometers, *Appl. Optics*, 35, 2787–2796, 1996.

10518

Gunson, M. R., Abbas, M. M., Abrams, M. C., Allen, M., Brown, L. R., Brown, T. L., Chang, A. Y., Goldman, A., Irion, F. W., Lowes, L. L., Mahieu, E., Manney, G. L., Michelsen, H. A., Newchurch, M. J., Rinsland, C. P., Salawitch, R. J., Stiller, G. P., Toon, G. C., Yung, Y. L., and Zander R.: The Atmospheric Trace Molecule Spectroscopy (ATMOS) experiment: Deployment on the ATLAS Space Shuttle missions, *Geophys. Res. Lett.*, 23, 2333–2336, 1996.

10523

Intergovernmental Panel on Climate Change (IPCC): Climate Change 2001: The Scientific Basis, Contribution of Working Group I to the Third Assessment Report of the Intergovernmental Panel on Climate Change, edited by J. T. Houghton et al., pp.944, Cambridge University Press, UK, 2001. [10516](#), [10527](#), [10528](#)

Irion, F. W., Brown, M., Toon, G., and Gunson, M. R.: Increase in Atmospheric CHF<sub>2</sub>Cl (HCFC–22) over Southern California from 1985 to 1990, *Geophys. Res. Lett.*, 21(16), 1723–1726, 1994. [10525](#)

Kanakidou, M., Dentener, F., and Crutzen, P.: A global three-dimensional study of the fate of HCFCs and HFC-134a in the troposphere, *J. Geophys. Res.*, 100(D9), 18 781–18 801, doi:10.1029/95JD01919, 1995. [10528](#)

Kerridge, B. J., Goutail, F., Bazureau, A., Wang, D.-Y., Bracher, A., Weber, M., Bramstedt, K., Siddans, R., Latter, B. G., Reburn, W. J., Jay, V. L., Dethof, A., and Payne, V. H.: MIPAS ozone validation by satellite intercomparisons, Proceedings of the ACVE-2 meeting, 3-7 May, Frascati, Italy, 2004. [10522](#)

Kleinert, A., Aubertin, G., Perron, G., Birk, M., Wagner, G., Hase, F., Nett, H., and Poulin, R.: MIPAS Level 1B algorithms overview: operational processing and characterization, *Atmos. Chem. Phys.*, 7, 1395–1406, 2007,

<http://www.atmos-chem-phys.net/7/1395/2007/>. [10519](#)

Lahoz, W., Geer, A., Swinbank, R., Jackson, D., Thornton, H., Dethof, A., and Fonteyn, D.: Modelling and assimilation: evaluation of MIPAS water vapour, Proceedings of the ACVE-2 meeting, 3–7 May, Frascati, Italy, 2004. [10522](#)

Miller, B. R., Huang, J., Weiss, R. F., Prinn, R. G., and Fraser, P. J. : Atmospheric trend and lifetime of chlorodifluoromethane (HCFC–22) and the global tropospheric OH concentration, *J. Geophys. Res.*, 103(D11), 13237–13248, 1998. [10517](#), [10525](#), [10527](#)

Molina, M. J., and Rowland, F. S.: Stratospheric sink for chlorofluoromethanes-chlorine atom catalyzed destruction of ozone, *Nature*, 249, 810–812, 1974. [10516](#)

ACPD

7, 10515–10541, 2007

## Growth rates of stratospheric HCFC-22

D. P. Moore and  
J. J. Remedios

Title Page

Abstract

Introduction

Conclusions

References

Tables

Figures

⏪

⏩

◀

▶

Back

Close

Full Screen / Esc

Printer-friendly Version

Interactive Discussion

**Growth rates of  
stratospheric  
HCFC-22**D. P. Moore and  
J. J. Remedios

Title Page

Abstract

Introduction

Conclusions

References

Tables

Figures

◀

▶

◀

▶

Back

Close

Full Screen / Esc

Printer-friendly Version

Interactive Discussion

Montzka, S. A., and Fraser, P. J.: Controlled substances and other source gases, Chapter 1 in Scientific Assessment of Ozone Depletion: 2002, World Meteorological Organization Global Ozone Research and Monitoring Project, Report No. 47, 1.1-1.83, WMO, Geneva, Switzerland, 2003. [10517](#)

5 Montzka, S. A., Myers, R. C., Butler, J. H., and Elkins, J. W.: Global tropospheric distribution and calibration scale of HCFC-22, *Geophys. Res. Lett.*, 20(8), 703–706, 1993. [10523](#)

Moore, D. P.: Measurements of HCFC-22 in the upper troposphere and lower stratosphere from the MIPAS-E instrument, PhD thesis, University of Leicester, 2005.

10 Moore, D. P., Waterfall, A. M., and Remedios, J. J.: The potential for radiometric retrievals of halocarbon concentrations from the MIPAS-E instrument, *Adv. Space. Res.*, 37, 2238–2246, 2006. [10519](#)

O'Doherty, S., Cunnold, D. M., Manning, A., Miller, B. R., Wang, R. H. J., Krummel, P. B., Fraser, P. J., Simmonds, P. G., McCulloch, A., Weiss, R. F., Salameh, P., Porter, L. W., Prinn, R. G., Huang, J., Sturrock, G., Ryall, D., Derwent, R. G., and Montzka S. A.: Rapid growth of hydrofluorocarbon 134a and hydrochlorofluorocarbons 141b, 142b, and 22 from Advanced Global Atmospheric Gases Experiment (AGAGE) observations at Cape Grim, Tasmania, and Mace Head, Ireland, *J. Geophys. Res.*, 109, D06310, doi:10.1029/2003JD004277, 2004. [10517](#), [10525](#)

15 Oelhaf, H., Blumenstock, T., De Mazière, M., Mikuteit, S., Vigouroux, C., Wood, S., Bianchini, G., Baumann, R., Blom, C., Cortesi, U., Liu, G. Y., Schlager, H., Camy-Peyret, C., Catoire, V., Pirre, M., Strong, K., and Wetzel, G.: Validation of MIPAS-ENVISAT version 4.61 HNO<sub>3</sub> operational data by stratospheric balloon, aircraft and ground-based measurements, Proceedings of the ACVE-2 meeting, 3–7 May, Frascati, Italy, 2004. [10522](#)

20 Plumb, R. A., and Ko, M. K. W.: Interrelationships between mixing ratios of long-lived stratospheric constituents, *J. Geophys. Res.*, 97, 10,145–10,156, 1992. [10527](#)

Remedios, J. J.: Extreme atmospheric constituent profiles for MIPAS, Proceedings of the European Symposium on atmospheric measurements from space, Vol. 2, ESTEC, Noordwijk, Netherlands, 20–22 Jan, 779–783, 1999. [10519](#), [10521](#), [10522](#)

25 Rinsland, C. P., Boone, C., Nassar, R., Walker, K., Bernath, P., Mahieu, E., Zander, R., McConnell, J. C. and Chiou, L.: Trends of HF, HCl, CCl<sub>2</sub>F<sub>2</sub>, CCl<sub>3</sub>F, CHClF<sub>2</sub> (HCFC-22), and SF<sub>6</sub> in the lower stratosphere from Atmospheric Chemistry Experiment (ACE) and Atmospheric Trace Molecule Spectroscopy (ATMOS) measurements near 30° N latitude, *Geophys. Res. Lett.*, 32, L16S03, doi:10.1029/2005GL022415, 2005a. [10518](#), [10519](#), [10526](#), [10529](#)

- Rinsland, C. P., Chiou, L. S., Goldman, A., and Wood, S. W.: Long-term trends in CHF<sub>2</sub>Cl (HCFC–22) from high spectral resolution infrared solar absorption measurements and comparison with in situ measurements, *J. Quant. Spectrosc. Ra.*, 90, 367–375, 2005b. [10517](#), [10525](#)
- 5 Rodgers, C.: Inverse methods for atmospheric sounding: theory and practice, World Sci., River Edge, N. J, 2000. [10520](#), [10522](#)
- Rothman, L. S., Barbe, A., Benner, D. C., Brown, L. R., Camy-Peyret, C., Carleer, M. R., Chance, K., Clerbaux, C., Dana, V., Devi, V. M., Fayth, A. Flaud, J. M., Gamache, R. R., Goldman, A., Jacquemart, D., Jucks, K. W., Lafferty, W. J., Mandin, J.-Y., Massie, S. T., Nemtchinov, V., Newnham, D. A., Perrin, A., Rinsland, C. P., Schroeder, J., Smith, K. M., Smith, M. A. H., Tang, K., Toth, R. A., Vander Auwera, J., Varanasi, P., and Yoshino, K.: The HITRAN molecular spectroscopic database: edition of 2000 including updates through 2001, *J. Quant. Spectrosc. Radiat. Transfer*, 82(1–4), 5–44, 2003. [10521](#)
- 10 Sihra, K., Hurley, M. D., Shine, K. P., and Wallington, T. J.: Updated radiative forcing estimates of sixty-five, halocarbons and non-methane hydrocarbons, *J. Geophys. Res.*, 106, 20 493–20 506, 2001. [10517](#)
- 15 Spang, R., Remedios, J. J., Kramer, L. J., Poole, L. R., Fromm, M. D., Müller, M., Aumgarten, G., and Konopka, P.: Polar stratospheric cloud observations by MIPAS on ENVISAT: detection method, validation and analysis of the northern hemisphere winter 2002/2003, *Atmos. Chem. Phys.*, 5, 679–692, 2005, <http://www.atmos-chem-phys.net/5/679/2005/>. [10522](#)
- 20 Spang, R., Remedios, J. J., and Barkley, M. P.: Colour indices for the detection and differentiation of cloud types in infrared limb emission spectra, *Adv. Space. Res.*, 33, 1041–1047, 2004. [10521](#)
- 25 Spivakovsky, C. M., Logan, J. A., Montzka, S. A., Balkanski, Y. J. Foreman-Fowler, M., Jones, D. B. A., Horowitz, L. W., Fusco, A. C., Brenninkmeijer, C. A. M., Prather, M. J., Wofsy, S. C., and McElroy, M. B.: Three-dimensional climatological distribution of tropospheric OH: Update and evaluation, *J. Geophys. Res.*, 105, 8931–8980, 2000. [10528](#)
- United Nations Environment Programme (UNEP): Handbook for the International Treaties for the Protection of the Ozone Layer, 4th ed., Ozone Secr., Nairobi, 1996. [10517](#), [10528](#)
- 30 Varanasi, P.: Absorption spectra of HCFC–22 around 829 cm<sup>-1</sup> at atmospheric conditions, *J. Quant. Spectrosc. Ra.*, 48, 205–219, 1992. [10518](#)
- Waugh, D. W., and Hall, T. M.: Age of stratospheric air: Theory, observations, and models, *Rev.*

---

**Growth rates of  
stratospheric  
HCFC-22**D. P. Moore and  
J. J. Remedios

---

Title Page

Abstract

Introduction

Conclusions

References

Tables

Figures

◀

▶

◀

▶

Back

Close

Full Screen / Esc

Printer-friendly Version

Interactive Discussion

---

**Growth rates of  
stratospheric  
HCFC-22**

D. P. Moore and  
J. J. Remedios

---

Title Page

Abstract

Introduction

Conclusions

References

Tables

Figures



Back

Close

Full Screen / Esc

Printer-friendly Version

Interactive Discussion

## Growth rates of stratospheric HCFC-22

D. P. Moore and  
J. J. Remedios

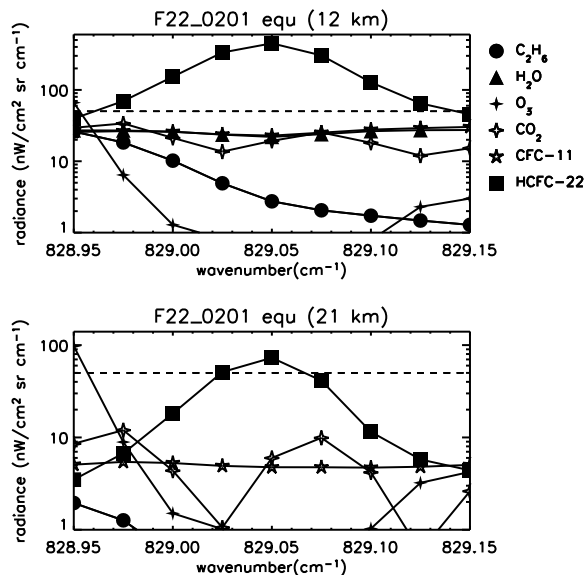
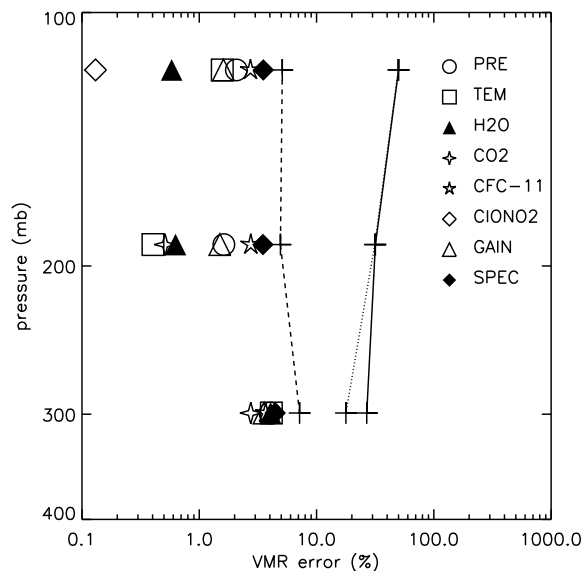


**Fig. 1.** Plot of modelled radiance contributions from the dominant radiatively active gases in the 828.95 to 829.15  $\text{cm}^{-1}$  range in the mid-latitudes (30 to 65 degrees). The black dotted line represents the expected noise equivalent spectral radiance (NESR) of the MIPAS-E which is based on pre-flight estimates of 50  $\text{nW}/(\text{cm}^2 \text{sr cm}^{-1})$  for band A.

[Title Page](#)
[Abstract](#)
[Introduction](#)
[Conclusions](#)
[References](#)
[Tables](#)
[Figures](#)
[⏪](#)
[⏩](#)
[◀](#)
[▶](#)
[Back](#)
[Close](#)
[Full Screen / Esc](#)
[Printer-friendly Version](#)
[Interactive Discussion](#)

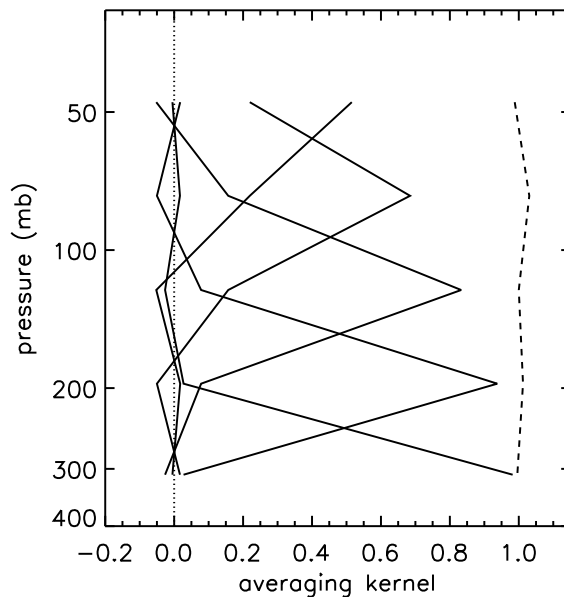
## Growth rates of stratospheric HCFC-22

D. P. Moore and  
J. J. Remedios



**Fig. 2.** Error budget for HCFC-22 vmr retrievals. The solid black line represents the total error on a single retrieval. The random (dotted) and systematic (dashed) component of the error are also shown. Systematic errors are dominated by gain, spectroscopic (“SPEC”), pressure (“PRE”), temperature (“TEM”) and CFC-11 uncertainties.

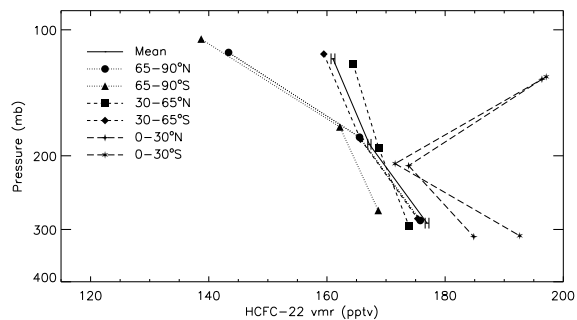
[Title Page](#)
[Abstract](#)
[Introduction](#)
[Conclusions](#)
[References](#)
[Tables](#)
[Figures](#)
[⏪](#)
[⏩](#)
[◀](#)
[▶](#)
[Back](#)
[Close](#)
[Full Screen / Esc](#)
[Printer-friendly Version](#)
[Interactive Discussion](#)

**Growth rates of  
stratospheric  
HCFC-22**D. P. Moore and  
J. J. Remedios

**Fig. 3.** Representative averaging kernels for a single mid-latitude HCFC-22 retrieval in 2003. There are almost four degrees of freedom for these five measurements. The highest peaks (i.e. the greatest amount of measurement information) are at higher pressures. The dashed black line represents the sum of the rows of the averaging kernel at each tangent pressure.

[Title Page](#)[Abstract](#)[Introduction](#)[Conclusions](#)[References](#)[Tables](#)[Figures](#)[⏪](#)[⏩](#)[◀](#)[▶](#)[Back](#)[Close](#)[Full Screen / Esc](#)[Printer-friendly Version](#)[Interactive Discussion](#)



**Growth rates of  
stratospheric  
HCFC-22**D. P. Moore and  
J. J. Remedios

**Fig. 4.** HCFC-22 vmr retrievals from 6434 converged profiles from 2003. Means by latitude band are also shown.

[Title Page](#)[Abstract](#)[Introduction](#)[Conclusions](#)[References](#)[Tables](#)[Figures](#)[◀](#)[▶](#)[◀](#)[▶](#)[Back](#)[Close](#)[Full Screen / Esc](#)[Printer-friendly Version](#)[Interactive Discussion](#)

## Growth rates of stratospheric HCFC-22

D. P. Moore and  
J. J. Remedios

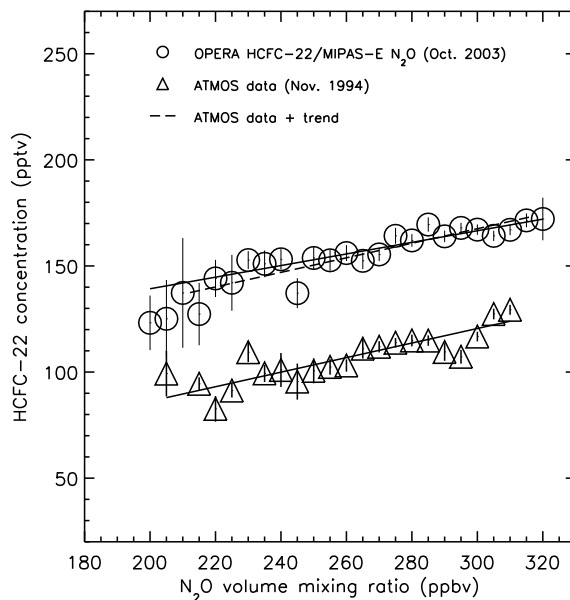


**Fig. 5.** ATMOS (AT-3, version 3) data and MIPAS-E data (version 4.61 for N<sub>2</sub>O) between 20° N and 50° N. Open triangles and open squares display averages in 5 ppbv N<sub>2</sub>O intervals. The one standard deviations of both the ATMOS and the OPERA derived HCFC-22 vmr data within each bin are also shown. The dashed black line represents the “expected” growth in both HCFC-22 and N<sub>2</sub>O since the ATMOS data in 1994 based on the observed trend in global average surface measurements made by ESRL since that time.

[Title Page](#)[Abstract](#)[Introduction](#)[Conclusions](#)[References](#)[Tables](#)[Figures](#)[◀](#)[▶](#)[◀](#)[▶](#)[Back](#)[Close](#)[Full Screen / Esc](#)[Printer-friendly Version](#)[Interactive Discussion](#)

## Growth rates of stratospheric HCFC-22

D. P. Moore and  
J. J. Remedios

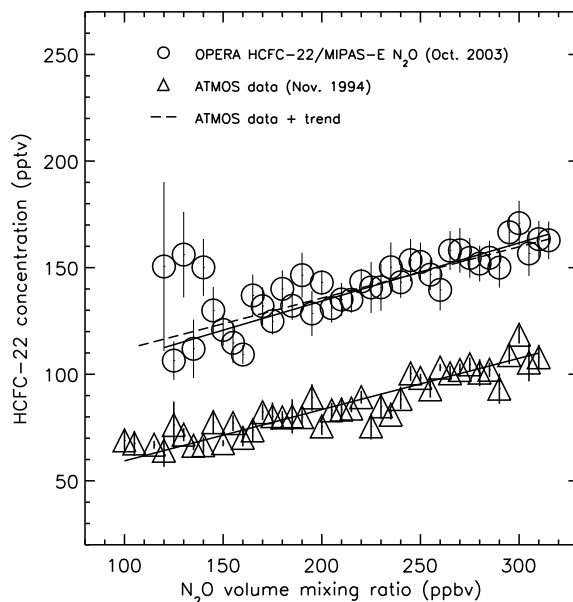


**Fig. 6.** ATMOS (AT-3, version 3) data and MIPAS-E data (version 4.61 for N<sub>2</sub>O) between 60° S and 80° S. Open triangles and open squares display averages in 5 ppbv N<sub>2</sub>O intervals. The one standard deviations of the OPERA derived HCFC-22 vmr data within each bin are also shown. The solid blue and red lines represent fits to the binned ATMOS and MIPAS-E data respectively. The solid black line represents the “expected” growth in both HCFC-22 and N<sub>2</sub>O since the ATMOS data in 1994 based on the observed trend in global average surface measurements made by CMDL since that time.

[Title Page](#)[Abstract](#)[Introduction](#)[Conclusions](#)[References](#)[Tables](#)[Figures](#)[◀](#)[▶](#)[◀](#)[▶](#)[Back](#)[Close](#)[Full Screen / Esc](#)[Printer-friendly Version](#)[Interactive Discussion](#)